

# Effect of acceleration on the wavy Taylor vortex flow

Q. Xiao, T. T. Lim, Y. T. Chew

639

**Abstract** In this paper, we use a laser optical technique to investigate the characteristics of a wavy Taylor vortex flow between two concentric cylinders, with the inner cylinder subjected to a wide range of predetermined acceleration and the outer one at rest. We focus on the inner/outer radius ratio of 0.894, with an acceleration ( $dRe/dt^*$ ) from 0.1123 to 2,247, and Reynolds number from  $Re/Re_c = 1.0$  to 36. The results show that, with increasing Reynolds number, there is an initial increase in the wavelength of the wavy vortex flow ( $\lambda$ ), and a decrease in the wave speed ( $c$ ) before they asymptote to a constant value, which is a function of the acceleration. As for the wave amplitude ( $A$ ), it is found that the effect of acceleration is significant only in a very narrow range of Reynolds numbers.

## 1 Introduction

Since the pioneering work of G.I. Taylor in 1923, Taylor–Couette flow has been the subject of intense theoretical and experimental investigations. A comprehensive review of the subject can be found in Koschmieder (1973), DiPrima and Swinney (1985), Kataoka (1986) and, more recently, Chossat and Iooss (1992).

One of the most conspicuous characteristics of the Taylor–Couette flow is the non-uniqueness of the wavy flow. This behaviour was first reported by Coles (1965), when he discovered the existence of 20–25 different flow states which have distinct axial wavelengths and/or azimuthal wavelengths for a given Reynolds number. He found that the flow states depend not only on the initial conditions, but also on the manner in which the inner cylinder was accelerated to the final speed. Since then, extensive works have been conducted to study this phenomenon. For example, Koschmieder (1979) used two acceleration procedures (which he referred to as “steady acceleration” and “sudden start”) to investigate the axial wavelength dependence on the acceleration. He found that, before the onset of turbulence, the axial wavelength of the Taylor vortices obtained by the “sudden start” condition

is, within experimental uncertainty, the same as that obtained by the “steady acceleration”. However, when the vortices become turbulent, their wavelengths are affected by changes in the initial conditions.

Apart from the axial and azimuthal wavelengths, the non-uniqueness of the wavy vortex flow is also reflected in the other two flow characteristics, namely wave speed and wave amplitude. The available literature concerning this aspect of the flow is rare, and the notable work is by King et al. (1984), who conducted an extensive study of the wave speed using both experimental and numerical methods. They found that, for a given Reynolds number, aspect ratio and radius ratio, the wave speed is a weak function of the acceleration procedure.

Compared with the axial wavelength and wave speed, the wave amplitude has not received much attention until recently. In 1985, Bust et al. (1985) investigated experimentally the dependence of the wave amplitude on the Reynolds number, based on a particular acceleration process in which the rotation rate of the inner cylinder is increased to a desired  $\omega$  within a specified time of half an hour to an hour. His results revealed a rapid increase in non-dimensional amplitude (normalised by axial average wavelength) in the range of  $1.2 < Re/Re_c < 2.2$ .

Although the non-uniqueness of the wavy vortex flow is well established, there are very few systematic investigations in which the effect of “flow history” is accurately quantified. Recently, we made an attempt in this direction by subjecting the inner cylinder to a wide range of linear acceleration and quantifying the “flow history” as  $dRe/dt^*$ . During the course of the experiment, we discovered a previously unidentified flow regime, which we referred to as “second Taylor vortex flow” or STVF. See Lim et al. (1998) and Xiao et al. (2002) This flow regime is found to be a function of not only the Reynolds number, but also of the acceleration. Because our earlier work was concentrated solely on axisymmetric Taylor vortices and the second Taylor vortices, we decided to extend the investigation to the wavy flow regime. The aim is to investigate how the axial wavelength, wave speed and wave amplitude of the wavy vortex flow are affected by changes in the linear acceleration. Here, we concentrate on the radius ratio of 0.894, and the acceleration ( $dRe/dt^*$ ) from 0.1123 to 2,247 and the Reynolds number from  $Re/Re_c = 1.0$  to 36.

The paper is organised as follows: the experimental facility and procedure are described in Sect. 2. This is followed by results and discussion in Sect. 3. Conclusions are presented in Sect. 4.

Received: 21 August 2001 / Accepted: 22 November 2001

Q. Xiao, T.T. Lim (✉), Y.T. Chew  
Department of Mechanical Engineering  
National University of Singapore  
10 Kent Ridge Crescent, Singapore 119260  
e-mail: mpelimt@nus.edu.sg

## 2 Experimental apparatus and procedure

The experimental apparatus used in the present investigation is similar to the one described in Lim et al. (1998) and is shown schematically in Fig. 1. It consists of a rotating inner cylinder with outer radius  $R_1$  of  $84.0 \pm 0.894$  mm and a stationary outer precision Perspex cylinder with an inner radius  $R_2$  of  $94.0 \pm 0.01$  mm. The aspect ratio ( $\Gamma = H/d$ ) and radius ratio ( $\eta = R_1/R_2$ ) are 94 and 0.894, respectively. Here,  $H$  is the height of the fluid column in-between the inner and the outer cylinders and  $d = (R_2 - R_1)$ . The inner cylinder is driven via a pair of bevel gears by a micro-stepper motor controlled by a PC. To ensure that the cylinders are accurately aligned with each other, the outer cylinder sits tightly in two circular recesses located on the top and bottom square plates, which also provide the anchor points for the four side panels. As for the inner cylinder, its bottom end is supported by a stainless shaft, which passes through the centre of the bottom plate, and its top end is connected to a brass bushing, which rotated freely inside a matching hole on the top plate.

The working fluid is a mixture of glycerin and water, and in order to achieve a wide range of Reynolds number ( $1.0 < Re/Re_c < 36$ ), we find it necessary to use two different glycerin/water mixtures of different kinematic viscosities ( $\nu = 11.60 \times 10^{-6} \text{ m}^2/\text{s}$  and  $6.234 \times 10^{-6} \text{ m}^2/\text{s}$ ). The viscosity ( $\nu$ ) of the mixture is measured by a HAAKE 75 Rheometer at a room temperature of  $27^\circ\text{C}$ . In all cases, one end of the fluid column is bounded by a stationary solid surface, while the other end is a free liquid surface. This configuration is similar to the one used by Cole

(1976) to investigate the annulus-length effects on Taylor-vortex instability. All the experimental data are conducted in an air-conditioned room, where the temperature variation is within  $0.5^\circ\text{C}$  throughout the experiment.

To visualise the flow, Kalliroscope AQ-100 reflective flakes are added to the solution and illuminated with five 30-W fluorescent lights and two spotlights. However, to visualise the cross section of the vortex structures, a 5-W argon ion laser expanded by an 8-mm cylindrical lens to attain a 2-mm-thick light sheet is used. Visual data are recorded using both still photography and video camera for subsequent analysis. To minimise possible heating of the working fluid by the laser, a minimum laser power (i.e. 2 W) is used, and is turned on only during the video recording. As stated earlier, the temperature variation is within  $0.5^\circ\text{C}$  throughout the experiment.

To measure the non-dimensional wave speed  $c = 2\pi f/m\Omega$ , where  $f$  is the frequency corresponding to the passage of the wave past a point of observation,  $m$  is the azimuthal wavy number, and  $\Omega$  is the angular velocity of inner cylinder, a laser-sectioning technique is used together with a video recorder equipped with time-coding facility. This is carried out by first generating a thin laser sheet using the technique described above, and the sheet is then positioned in an axial plane ( $r, z$ ) which allows vertical cross-sections of the flow to be made (see Fig. 1). When wavy vortices appear, their motion in the azimuthal direction is manifested as a vertical oscillating wave in the plane of the laser sheet. By replaying the video flow images frame by frame, the period of oscillation, and hence the wave frequency can be easily determined. Using velocity power

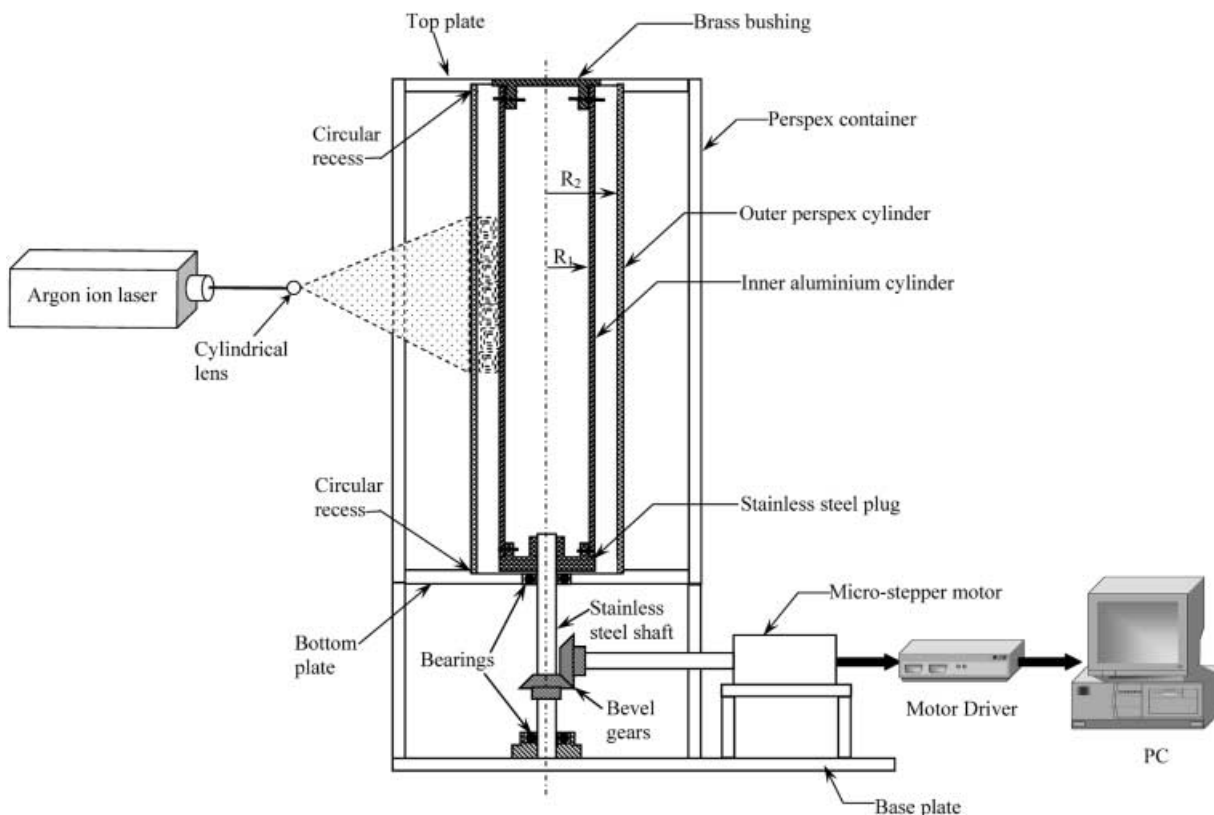


Fig. 1. A schematic drawing of the experimental set-up

spectra measurements, King et al. (1984) found that the wavy vortex flow consists of a single frequency, which is equal to the frequency with which the waves pass through a given point. The laser optical method used in the present study is proven to be accurate when compared with the power spectra measurements of King et al. (1984).

Because of the ends effect, the cell size along the column is usually non-uniform, therefore the *average* axial wavelength  $\lambda = 2H/Nd$ , where  $H$  is the height of the column, and  $d$  is the gap width between two cylinders, is selected for characterising the flow. The key parameter in the axial average wavelength measurement is the axial wave number. Here, it is measured by counting the total number of vortices  $N$  along the height of the fluid column. To ensure sufficient data convergence, each experiment is repeated at least 10 times, and the number  $N$  of vortices is then averaged from the integer number of vortices observed in each realisation. Note that, although the cell size along the fluid column may not be non-uniform, the maximum percentage variation in  $\lambda$  along the length of the annulus is only 4.61% for this particular radius ratio.

The wave amplitude ( $A$ ) is defined as half the vertical distance between crests and troughs of a wave. To measure the wave amplitude and azimuthal wavelength, an accurately drawn orthogonal grid (or scale) made from transparency paper is fixed onto the external surface of the outer Perspex cylinder, along the azimuthal direction. The flow motion is recorded with full view of the scale. When the flow images are replayed frame by frame, the scale enables the azimuthal wavelength as well as the wave amplitude to be measured.

The two controlling parameters in the present investigation are the Reynolds number ( $Re = R_1\Omega d/\nu$ ), and the linear acceleration ( $dRe/dt$ ). Non-dimensionally, linear acceleration is defined  $dRe/dt^* = (R_1d/\nu) d\Omega/dt^*$ , where  $t^*$  is a non-dimensional time defined as  $tv/d^2$ , keeping in mind that  $d^2/\nu$  is the radial diffusion time. In all cases, only the inner cylinder is subjected to the constant acceleration, typically from rest to a desired speed ( $\Omega$ ) over a predetermined time-interval using the above PC controlled stepper motor. For ease of reference, the most upper limit of the acceleration is referred to as the “sudden start” condition and the lower limit is referred to as “quasi-steady” condition. Note that the upper limit is dictated by the inertia of the rotating system and the torque of the stepper motor, while the lower limit refers to the condition below which the flow characteristics are independent of the acceleration.

It is important to note that each of the data points presented here is obtained usually more than 2 h after the final rotation speed is reached, which is equivalent to about 580 times its radial diffusion time ( $d^2/\nu$ ). To avoid a possible “memory effect” in the fluid, a break of at least 1 h is allocated between each run, and most of the experiments are repeated, at least one day apart, to ensure that the results are reproducible.

By using the error analysis discussed in Holman (1989), the experimental uncertainties for Reynolds number is  $\delta Re = 2.55\%$ , and linear acceleration is  $\delta\left(\frac{dRe}{dt^*}\right) = 3.6\%$ . Similarly, the uncertainty for the axial wavelength ( $\lambda$ ) is

$\delta_\lambda = 2.13\%$ , wave speed is  $\delta_c = 2.66\%$  and the non-dimensional wave amplitude ( $\bar{A} = \frac{A}{d}$ ) is  $\delta\bar{A} = 1.2\%$ .

### 3 Results and discussion

Figure 2 shows the effect of acceleration on the axial wavelength of the wavy vortex flow under the following acceleration conditions:  $dRe/dt^* = 0.112, 1.12, 11.2$  and  $2,247$ . Included in the same plot are the results of Koschmieder (1979) for the purpose of comparison.

Referring to our results first, it is obvious from the figure that the axial wavelength is a function of both the acceleration and the Reynolds number. Within the Reynolds number range of  $1.0 < Re/Re_c < 10.0$ , it increases monotonically with the Reynolds number and at the same time is independent of the imposed acceleration. Visual results for the same Reynolds number range show that the flow remains laminar and follows the classical transition sequence of CCF  $\Rightarrow$  TVF  $\Rightarrow$  WVF as the Reynolds number increases. A detailed observation indicates that the transition from TVF to WVF occurs over a very narrow range of  $1.00 < Re/Re_c < 1.12$ . Beyond  $Re/Re_c = 1.12$ , the flow is wavy with the azimuthal wave number of  $m=3$ , and a further increase in the Reynolds number to  $Re/Re_c \approx 3.7$  leads to a change in the wave number from  $m = 3$  to  $m = 6$ . From here, the flow remains in the same state ( $m = 6$ ) until it reverts back to  $m = 3$  when  $Re/Re_c \approx 10$ . Figure 3a–c shows the corresponding visual results of

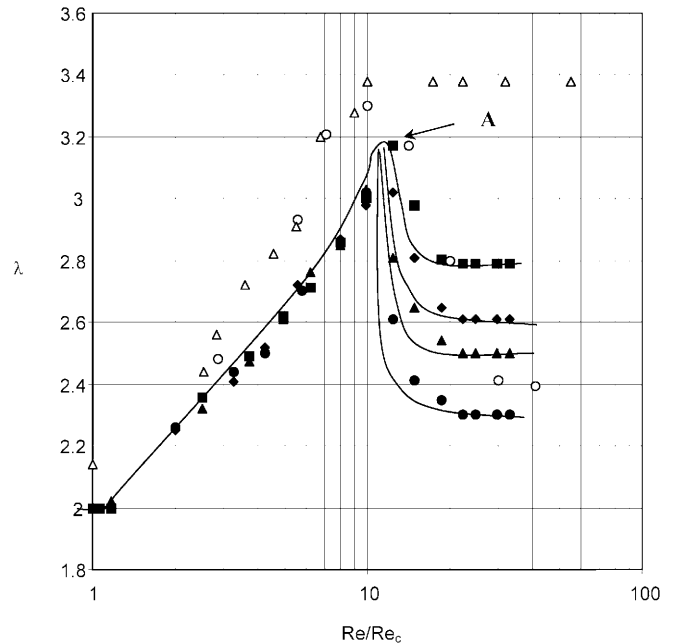
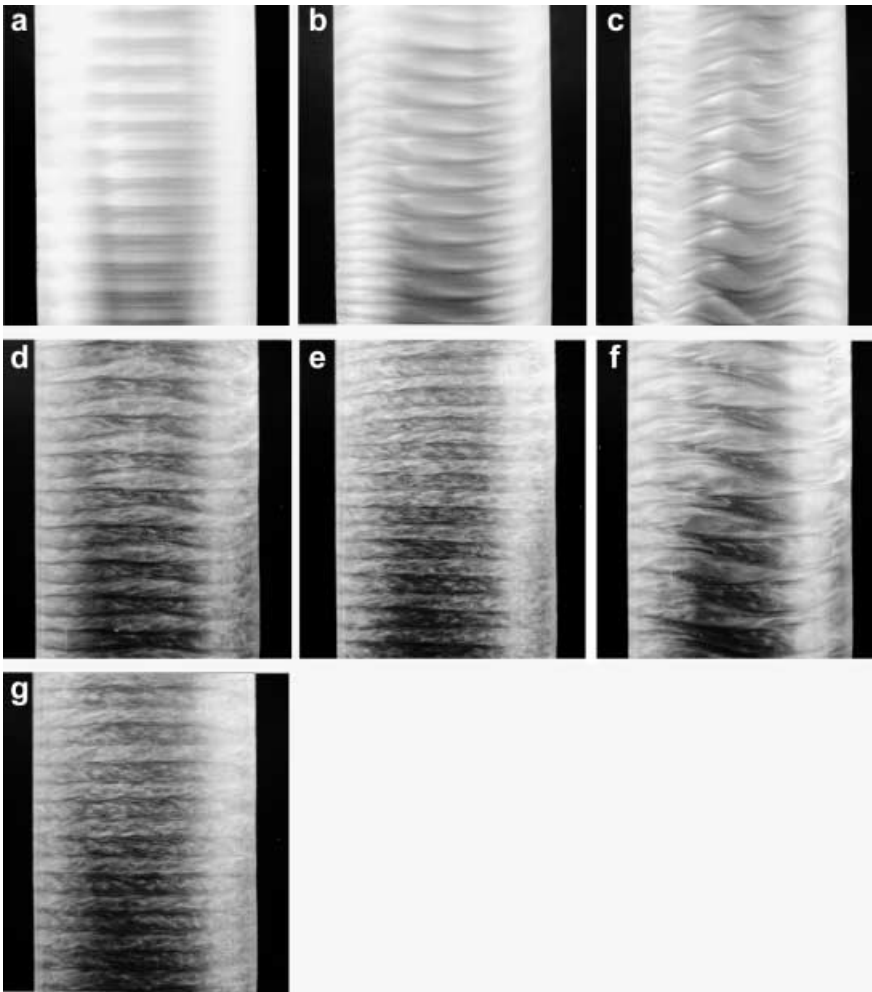


Fig. 2. Effect of acceleration on the relationship between axial wavelength and Reynolds number: A comparison with Koschmieder (1979). Our results,  $\eta = 0.894$ ,  $\Gamma = 94$ : filled squares,  $dRe/dt^* = 0.1123$ ; filled diamonds,  $dRe/dt^* = 1.123$ ; filled triangles,  $dRe/dt^* = 11.23$ ; filled circles,  $dRe/dt^* = 2,247$ . Results of Koschmieder,  $\eta = 0.890$ ,  $\Gamma = 123.5$ : open triangles, quasi-steady; open circles, sudden start. Note that the peak wavelength (indicated by A) occurs at the onset of turbulent wavy vortex flow ( $m = 3$ )



**Fig. 3a-g.** Photographs showing the flow between concentric cylinders with the inner cylinder rotating: **a-e**  $dRe/dt = 2,247$ ; **f-g**  $dRe/dt = 0.1123$ ; **a**  $Re/Re_c \approx 1.0$ , Taylor vortex flow,  $\lambda = 2.0$ ; **b**  $Re/Re_c = 2.0$ , laminar wavy vortex flow with  $m = 3$ ,  $\lambda = 2.21$ ; **c**  $Re/Re_c = 4.0$ , laminar wavy vortex flow with  $m = 6$ ,  $\lambda = 2.54$ ; **d**  $Re/Re_c = 12.5$ , turbulent wavy vortex flow with  $m = 3$ ,  $\lambda = 2.61$ ; **e**  $Re/Re_c = 26.0$ , turbulent axisymmetric Taylor vortex flow,  $\lambda = 2.3$ ; **f**  $Re/Re_c = 12.5$ , turbulent wavy vortex flow with  $m = 3$ ,  $\lambda = 3.18$ ; **g**  $Re/Re_c = 26.0$ , turbulent axisymmetric Taylor vortex flow,  $\lambda = 2.79$

Taylor vortices at  $Re/Re_c \approx 1.0$ , wavy vortex flow ( $m = 3$ ) at  $Re/Re_c = 2.0$  and wavy vortex flow ( $m = 6$ ) for  $Re/Re_c = 4.0$ .

When the Reynolds number is increased to about 11.5, weak turbulent Taylor vortices emerged. This finding agrees well with the result of Fenstermacher et al. (1979) ( $\eta = 0.877$ ,  $\Gamma = 20$ ), which also indicates the onset of turbulence in the Taylor vortices at  $Re/Re_c \approx 12$ . Likewise, Koschmieder's (1979) ( $\eta = 0.896$ ,  $\Gamma \approx 123$ ) results also show a similar transition to turbulence at about  $Ta/Ta_c \approx 100$  (which translates into  $Re/Re_c \approx 10$ ). As is clearly depicted in Fig. 2, the axial wavelength reaches a maximum when  $Re/Re_c \approx 11.5$  and, beyond here, it decreases rapidly with an increase in the Reynolds number before it asymptotes to a constant value. Visual observation for those cases above  $Re/Re_c \approx 11.5$  shows that the azimuthal wave number changes from  $m = 3$  to  $m = 2$  at  $Re/Re_c \approx 20$ , and finally to  $m = 0$  when  $Re/Re_c \approx 23.2$ . Obviously,  $m = 0$  indicates the presence of an axisymmetric turbulent TVF. This flow state persists for up to  $Re/Re_c = 36$ , which is the highest Reynolds number considered in this study. The flow visualisation pictures for the turbulent wavy vortex flow ( $m = 3$ ) at  $Re/Re_c = 12.5$  and turbulent axisymmetric Taylor vortex flow at  $Re/Re_c = 26$  under "sudden start" and "quasi-steady" conditions are shown in Fig. 3d-g.

Before comparing our results with those of Koschmieder (1979), it should be noted that the axial wavelength obtained by Koschmieder covers a much wider range of Reynolds number which extends from the onset of TVF to axisymmetric turbulent TVF (i.e. from  $Ta/Ta_c = 1.0$  to 4,000 which translates into  $Re/Re_c = 1.0$  to 63.24). However, his acceleration is limited to two extreme conditions only (i.e. "sudden start" and "steady acceleration" conditions). In addition, his radius ratio ( $\eta$ ) is 0.890 and the aspect ratio ( $\Gamma$ ) is 123.5 (compared with  $\eta = 0.894$  and  $\Gamma = 94$  in the present study). Nevertheless, previous studies have shown that for aspect ratio  $\Gamma > 30$ , the effect of aspect ratio is small. As to his "steady acceleration" condition, the actual acceleration used by him was  $7 \times 10^{-4} \text{ rad/s}^2$ . Based on the two different viscosities of his working solutions, this corresponded to the acceleration of  $dRe/dt^* = 0.017$  and 0.1224. Also, Koschmieder defined the "sudden start" condition as the process in which the final Reynolds number is achieved within 1 s. It can be seen from Fig. 2 that the two sets of results generally follow the same trend until the onset of weak turbulence at  $Re/Re_c > 10$ . Within this Reynolds number range, both sets of results exhibit increasing axial wavelength with the Reynolds number, regardless of the acceleration. However, beyond the Reynolds number of  $Re/Re_c \approx 11.5$ , the axial wavelengths in the two studies show a

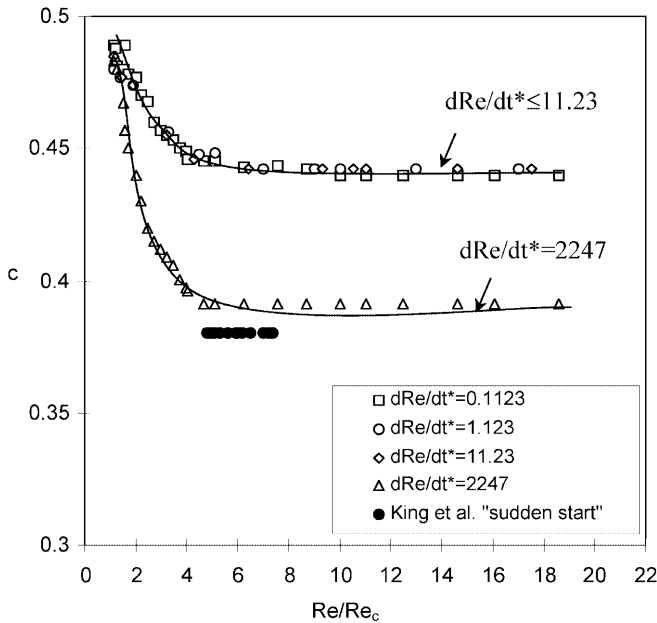


Fig. 4. Effect of acceleration on the relationship between wave speed and Reynolds number. Note that for  $dRe/dt^* \leq 11.23$ , all the wave speeds collapse onto a single curve, thus indicating that they are independent of the acceleration below 11.23

rather strong acceleration dependence with the small axial wavelength corresponding to the large imposed acceleration. For reasons which are not entirely clear, our axial wavelengths before the onset of turbulent wavy vortex flow are somewhat lower than those of Koschmieder. Repeatable studies by us confirm our finding. In addition, for the Reynolds number beyond the onset of turbulent wavy vortex flow, there is a distinct difference between his “quasi-steady” results and ours. While Koschmieder’s results show the axial wavelength to be independent of the Reynolds number, our result indicates a rather abrupt decrease in the wavelength with the Reynolds number before it asymptotes to a constant value, which is considerably lower than that of Koschmieder.

In Fig. 4, the relationship between the wave speed and the Reynolds number for the acceleration from  $dRe/dt^* = 0.1123$  to 2,247 is presented. For the purpose of comparison, the results of King et al. (1984) are also included. It can be seen from Fig. 4 that for the acceleration condition of  $dRe/dt^* \leq 11.23$ , all the present data collapse onto a single curve, which obviously indicates that the flow is independent of the acceleration. Nevertheless, within this acceleration range, the wave speed first decreases sharply with the Reynolds number before it asymptotes to a constant at around  $Re/Re_c = 4.5$ . Likewise for  $dRe/dt^* = 2,247$ , although the general trend is the same as above, the asymptotic value of the wave speed, however, is somewhat lower. In fact, the difference between the two asymptotic values is about 12%.

A comparison with the results of King et al. (1984) in Fig. 4 shows that our results for  $dRe/dt^* = 2,247$  are in reasonable agreement with King et al.’s, although our values are slightly larger. However, one should keep in mind that King et al. used a different criterion in determining the functional relationship between the Reynolds

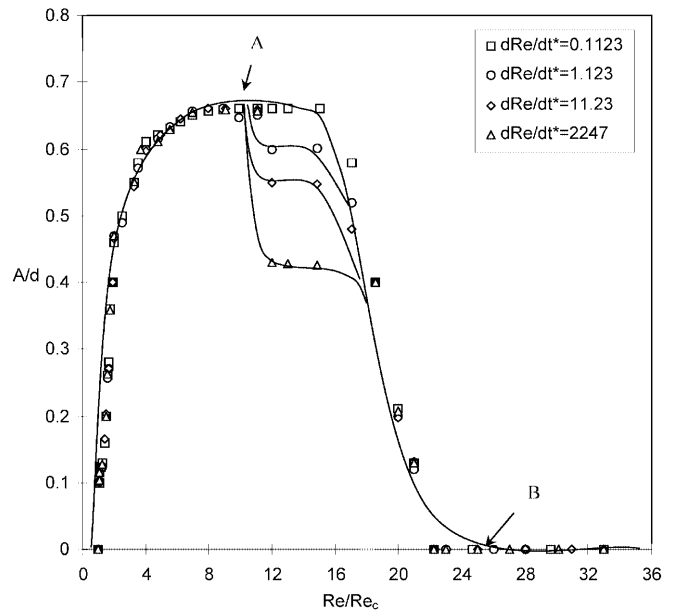
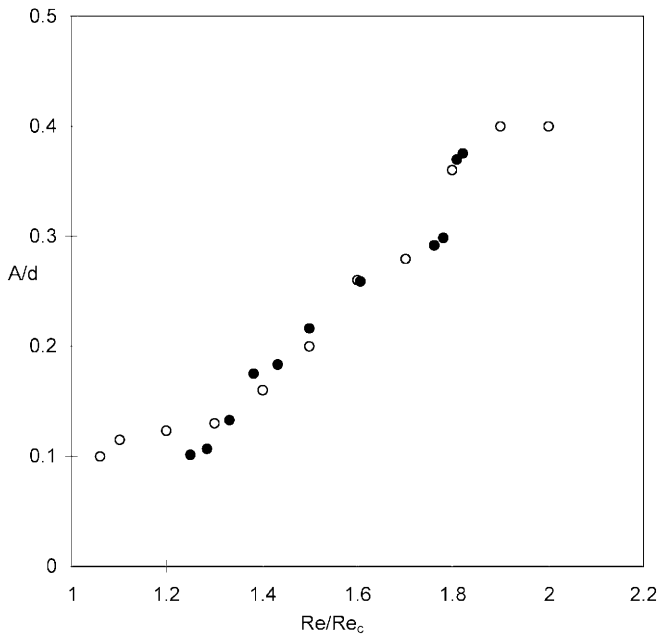


Fig. 5. Effect of acceleration on the relationship between wave amplitude and Reynolds number. Symbol A indicates the onset of turbulent WVF ( $m = 3$ ) at  $Re/Re_c \approx 11.5$ ; and the symbol B indicates the onset of axisymmetric turbulent TVF at  $Re/Re_c \approx 25.6$ . Note that before the onset of turbulence, the wave amplitudes under different acceleration coincide with each other

number and the wave speed. The criterion is based on the condition of “same axial wavelength” where neither the accelerating conditions was fixed, nor the exact acceleration with which the flow was subjected to specified, as long as the “same axial wavelength” is achieved. However, they did mention that “the system was started suddenly from rest to a desired wave number”. In contrast, we used a predetermined “acceleration” to achieve a predetermined final Reynolds number. Based on the flow conditions given by them, the only meaningful comparison of their results can be drawn with our results of the highest acceleration (i.e.  $dRe/dt^* = 2,247$ ).

Figure 5 displays the acceleration effect on the wave amplitude versus the Reynolds number for the same acceleration range as above (i.e.  $dRe/dt^* = 0.1123, 1.123, 11.23$  and 2,247). For the purpose of the discussion here, we use the results of  $dRe/dt^* = 2,247$  as a reference. Here, it can be seen that the wave amplitude initially increases rapidly with the Reynolds number, before it asymptotes to a constant value of 0.66, and stays unchanged until the flow reaches a transitional Reynolds number of  $Re/Re_c \approx 11.5$ . Beyond here, the wave amplitude drops sharply to about 0.43, and remains constant for a narrow Reynolds number range, before it declines to zero. It is worth pointing out that up to the transitional Reynolds number, only laminar wavy vortex flow is found to exist. However, above the transitional Reynolds number, our flow visualisation results indicate a rapid transition from the laminar wavy vortex flow to a turbulent wavy vortex flow.

As for the wave amplitude of the other low acceleration cases, it is clear from the figure that the results follow the same trend as that for  $dRe/dt^* = 2,247$ , except at the transitional Reynolds number of around 11.5, where the



**Fig. 6.** Relationship between the wave amplitude of wavy vortex flow and the Reynolds number; a comparison with Bust et al. (1985). Bust et al. (1985),  $\eta = 0.8848$ ,  $\Gamma = 30.02$ ,  $m = 4$ ,  $\lambda = 2.01$ , open circles; present results:  $\eta = 0.8936$ ,  $\Gamma = 94$ ,  $m = 3$ ,  $\lambda = 2.0$ , filled circles

extent of the drop in the wave amplitude depends very much on the acceleration: a high acceleration leads to a large reduction in the wave amplitude.

It is worth noting that the variation of the wave amplitude with the Reynolds number has also been investigated by Bust et al. (1985). In their study, the rotating speed of the inner cylinder was increased slowly and steadily from zero up to the desired Reynolds number. However, their results were restricted to a very narrow range of Reynolds number from  $Re/Re_c = 1.2$  to 1.8 (see Fig. 6); compared with ours from  $Re/Re_c = 1.2$  to 36. Nevertheless, within the narrow range of the Reynolds number that they have investigated, our results compare well with theirs (see Fig. 6).

#### 4

#### Conclusions

We carried out a systematic study on the effect of linear acceleration on the axial wavelength, wave speed and wave amplitude of wavy Taylor vortex flow. Based on the results obtained for the acceleration ( $dRe/dt^*$ ) from 0.1123 to 2,247 and the Reynolds number from  $Re/Re_c = 1.0$  to 36, the following conclusions can be made. It is found that, in

addition to the Reynolds number, the axial wavelength, wave speed and wave amplitude of wavy Taylor vortex flow is a function of the acceleration. For example, the axial wavelength ( $\lambda$ ) is found to increase monotonically with the Reynolds number and at the same time is independent of the acceleration as long as  $Re < 10Re_c$ . Above  $Re \approx 11Re_c$ ,  $\lambda$  decreases with the Reynolds number before it asymptotes to a constant value which depends on the acceleration: the higher the acceleration, the lower is the asymptotic value. As for the wave speed ( $c$ ), it is also found to be a function of the Reynolds number, with the wave speed initially decreasing with Reynolds number before it also asymptotes to a constant value. Also, it appears that there is a certain threshold acceleration below which  $c$  is independent of the acceleration. Once above the threshold value, the asymptotic value of  $c$  is lower. As for the wave amplitude ( $A$ ), the effect of acceleration is significant only in a very narrow range of the Reynolds numbers. Outside this range, the wave amplitude is not affected by changes in the acceleration.

#### References

- Bust GS, Dornblaser BC, Koschmieder EL (1985) Amplitudes and wavelengths of wavy Taylor vortices. *Phys Fluids* 28:1243–1247
- Chossat P, Iooss G (1992) *The Couette–Taylor problem*. Springer, Berlin Heidelberg New York
- Cole JA (1976) Taylor-vortex instability and annulus-length effects. *J Fluid Mech* 75:1–15
- Coles D (1965) Transition in circular Couette flow. *J Fluid Mech* 21:385–425
- DiPrima RC, Swinney HL (1985) Instability and transition in flow between concentric rotating cylinders. In: Swinney HL, Gollub JP (eds) *Hydrodynamic instabilities and the transition to turbulence*, 2nd edn. Topics in applied physics, vol 45. Springer, Berlin Heidelberg New York, pp 139–180
- Fenstermacher PR, Swinney HL, Gollub JP (1979) Dynamical instabilities and the transition to chaotic Taylor vortex flow. *J Fluid Mech* 94:103–128
- Holman JP (1989) *Experimental methods for engineers*, 5th edn. McGraw-Hill, New York
- Kataoka K (1986) Taylor vortices and instability in circular Couette flow. In: Cheremisinoff NP (ed) *Encyclopedia of fluid mechanics*, vol 1. Gulf, Houston, p 236
- King GP, Li Y, Lee W, Swinney HS, Marcus PS (1984) Wave speeds in wavy Taylor-vortex flow. *J Fluid Mech* 141:365–390
- Koschmieder EL (1973) Taylor vortex flow. In: Benard cells and Taylor vortices. Cambridge University Press, New York
- Koschmieder EL (1979) Turbulent Taylor vortex flow. *J Fluid Mech* 93:515–527
- Lim TT, Chew YT, Xiao Q (1998) A new flow regime in a Taylor–Couette flow. *Phys Fluids* 10:3233–3235
- Xiao Q, Lim TT, Chew YT (2002) Second Taylor–Couette flow: effects of radius ratio and aspect ratio. *Phys Fluids* 14:1537–1539